ACS OMEGA

Open Access

http://pubs.acs.org/journal/acsodf

Article

High-Efficiency Adsorption of Uranium from Wastewater Using Graphene Oxide/Graphene Oxide Nanoribbons/Chitosan Nanocomposite Aerogels

Ali A. Jabbar, Dhia H. Hussain, Kamal H. Latif, Adel Kareem Jasim,* Zaidon T. Al-aqbi,* Hussein S. Alghannami, and Abdulkarim Albishri

Cite This: *ACS Omega* 2024, 9, 27260−27268

Read Online

ACCESS | Metrics & More | Article Recommendations

ABSTRACT: A chemical exfoliation and freeze-drying technique was used to create graphene oxide/graphene oxide nanoribbons/chitosan aerogels (GO/GONRs/CS). Aerogels were utilized to study uranium adsorption through batch experiments. Environmental influences on U(VI) adsorption were studied, including the starting concentration of U(VI), contact time, pH, and temperature. In order to characterize the composite, FTIR, SEM, XRD, and TEM analyses were used. A pseudo-second-order kinetic model may adequately represent the kinetics of U(VI) adsorption onto the surface of aerogels. The Freundlich model can explain the adsorption isotherm; the maximal adsorption capacity for U(VI) was determined to be 1208.85 mg/g; the adsorption process for U(VI) was endothermic, spontaneous, and pH-dependent; and the mechanism of adsorption is the chemisorption process. Chemisorption typically involves strong chemical interactions between the adsorbate (uranium ions) and the functional groups present on the surface of the adsorbent (the aerogel). Graphene oxide and graphene oxide nanoribbons contain oxygen-containing functional groups such as carboxyl (−COOH), hydroxyl (−OH), and epoxy (−O−) groups, which can act as active sites for chemical bonding. Chitosan, a polysaccharide derived from chitin, also possesses functional groups like amino ($-NH_2$) and hydroxyl groups. Uranium ions, in their U(VI) form, can form chemical bonds with these functional groups through various mechanisms such as electrostatic interactions, complexation, and coordination bonds. The combination of graphene oxide-based materials and chitosan in the nanocomposite aerogel offers several advantages, including a large specific surface area, chemical stability, and the presence of functional groups for effective uranium adsorption.

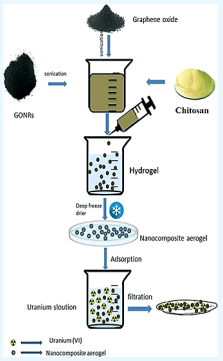

INTRODUCTION

Every year, radioactive wastewater including mining extraction of uranium, scientific research, and reactors causes significant ecological and environmental issues.[1,2] Many techniques have been used to remediate radioactive wastewater, including chemical processes like ion exchange, precipitation, extraction, biological degradation, and adsorption.[3,4] For separating radioactive elements, adsorption is considered one of the more successful approaches. According to the adsorption theory, various radioactive elements may be chemically and physically adsorbed by materials, and materials with a porous structure and a large surface area accelerate the process. In this concept, microporous and mesoporous materials, foam or sponge, and hydrogels have been utilized to purify radioactive elements from wastewater.[5] Due to their unusual physico-chemical features, such as a large specific surface area, great chemical stability, and an abundance of functional groups containing oxygen, graphene oxide (GO)-based nanomaterials have received considerable attention.[6,7] These characteristics make GO-based nanoparticles intriguing candidates for uranium adsorption. Graphene oxide nanoribbons/chitosan nanocomposite was appropriate for isolating uranium from wastewater and recovering it.[8] On the surface and margins of GO are several functional groups, including hydroxyl, epoxy, carboxyl, and carbonyl.[9,10] Due to these functional groups containing oxygen, GO is a perfect support material to combine with other chemical functional groups or composites due to its high dispersion, hydrophilicity, and compatibility. For environmental contaminants such as uranium and other radioactive species in wastewater, functional groups of graphene oxide may be employed as effective adsorption sites. The functional groups on GO and the experimental conditions have a significant impact on the uranium adsorption capacity of GO-based nanomaterials. Many publications show that pristine GOs have varied adsorption capabilities owing to diverse synthesis processes and factors influencing adsorption.[11] Furthermore, different modification approaches may typically increase the adsorption capabilities of modified GOs,

Received: February 19, 2024
Revised: May 30, 2024
Accepted: May 31, 2024
Published: June 13, 2024

which might be related to improved stability and dispersion, as well as the presence of additional functional groups and surface effective sites.

Chitosan (CS), a natural biopolymer obtained from the deacetylation of chitin, exhibits biocompatibility and biodegradability, making it an environmentally friendly option for various applications, such as wastewater treatment.[12] Moreover, due to its possession of amino and hydroxyl functional groups, chitosan has the ability to form chelation complexes and engage in electrostatic interactions with metal ions, including uranium. Consequently, chitosan can effectively adsorb and eliminate metal ions from the solution. By combining graphene oxide (GO) with chitosan (CS), the unique properties of both materials synergistically contribute to the development of an adsorbent with enhanced characteristics. The introduction of a 3D network formation of chitosan, through its combination with other materials like GO, further enhances the stability and mechanical strength of the adsorbent, thereby improving its effectiveness in adsorbing uranium and other contaminants.[13]More recently, we synthesized graphene oxide, graphene oxide nanoribbons, and sodium alginate nanocomposite aerogels (GO/GONRs/SA) using hydrothermal and lyophilization treatment in order to remove uranium from simulated wastewater.[14] Here, graphene oxide, GONRs, and chitosan were employed to increase the adsorption capacity and hydrophobicity, which is considered a development of our previous research. Sodium alginate was replaced with chitosan to study the effect of this change on the adsorption capacity, given that chitosan possesses functional groups different from sodium alginate.[14] Therefore, the goal of this work was to synthesize a GO/GONRs/CS aerogel using chemical exfoliation and lyophilization process in order to remove uranium from simulated wastewater. The shape and surface properties of the materials were examined by using various approaches, and the efficiency of aerogels in adsorbing uranium from aqueous solutions was evaluated.

EXPERIMENT

Materials. As a precursor, graphite powder (99% purity, Chemical Reagent from China) was used to produce graphene oxide (GO). Graphene oxide nanoribbons (GONRs) were generated using multiwalled carbon nanotubes (MWCNTs, Cheap Tube Inc., USA). Potassium permanganate ($KMnO_4$, BDH) served as an oxidant in the production of GONRs and GO. From uranyl nitrate ($(UO_2(NO_3)_2{\cdot}6H_2O$, solid 98−102% BDH, England), 1 g/L stock solutions of uranium were produced. 2.109 g of uranyl $UO_2(NO_3)_2{\cdot}6H_2O$ was dissolved in deionized water containing 1 mL of concentrated HNO_3. In a 1 L standard flask, the solution was diluted with deionized water until the mark is reached. The supplier of chitosan (CS) was Grantham Life Sciences UK). Analytical-grade supplementary reagents and deionized water were utilized to prepare all of the solutions.

Preparation of GO/GONRs/CS Aerogels. Graphene oxide (GO) was prepared by a combination of H_2SO_4 and H_3PO_4 with a volume ratio of 9:1 (180:20 mL). The liquid was agitated for 15 min before the addition of 1.5 g of graphite powder. Next, 9.0 g of $KMnO_4$ was added gently while the mixture was swirled continuously. The mixture was stirred constantly for 12 h. To stop the process after 12 h, 4 mL of 30% hydrogen peroxide (H_2O_2) was added with 200 mL of freezing deionized water, and then the solution was colored brilliant yellow. For purification, the mixture was divided into many centrifuge tubes. For each washing step, cleaning was carried out by switching between 10% hydrochloric acid (HCl) and deionized (DI) water, centrifuging at 5000 rpm for 15 min. After that, the finished product was dried in an oven set to 80 °C for 24 h.[15]

Unzipping multiwalled carbon nanotubes was used to create GONRs preoxidizing MWCNTs (1 g) in 150 mL of concentrated sulfuric acid at room temperature for 6 h, while stirring continuously was a usual procedure. After adding 500 wt % $KMnO_4$, the reaction mixture was agitated for an hour at room temperature. The mixture was heated at 55 °C for 30 min. After being brought up to 70 °C, the reaction mixture was allowed to stabilize for a while before being allowed to cool to room temperature. After adding the mixture to 400 mL of ice and mixing it with 5 mL (10%) of H_2O_2, the mixture was filtered through a PTFE membrane (0.5 μm). The substance was diluted in 120 mL of deionized water and then sonicated for 30 min. Following a PTFE membrane filtering of the mixture, the filtrate was dried at 60 °C for 24 h.[15−17]

The dried GO of 0.32 g (8 mg/mL) and GONRs of 0.32 g (8 mg/mL) were evenly dispersed in 20 mL of 2% acetic acid by ultrasonication for 1 h and then mixed with 20 mL of (1 g) CS solution (25 mg/mL) also in 2% acetic acid.[18] The GO/GONRs/CS suspension combination was then transferred to a 20 mL syringe (needle diameter: 0.8 mm) and added to 1 M NaOH solution at a controlled rate of injection (5 mL/h). The GO/GONRs/CS hydrogel beads were vacuum-freeze-dried for 72 h after being rinsed with deionized water five times.[19−21]

Adsorption Experiments. A predetermined quantity of the GO/GONRs/CS aerogel was added to a uranium solution for uranium adsorption investigations. The adsorbent (aerogel) was then extracted using centrifugation, and after that, the supernatant was examined by ED-XRF (Rigaku, USA). The removal rate (p) and the adsorption capacity (q_e) were calculated using the following equation:

$$q_e = \frac{(C_o - C_e) \times V}{M} \quad (1)$$

$$p = \frac{(C_o - C_e)}{C_o} \times 100\% \quad (2)$$

where V (mL) is the uranium volume, M (mg) is the dose of GO/GONRs/CS aerogel, and C_0 (mg/L) and C_e (mg/L) refer to uranium concentrations for the initial and adsorption equilibrium, respectively.

Characterization. Using SEM, TEM, FT-IR spectroscopy, and XRD, the materials were characterized. To generate SEM pictures, the SEM measurements were performed using a TESCAN MIRA3 French scanning electron microscope with a 15 kV electron beam. Using a BRUKER TENSOR 35 spectrophotometer 65, in pressed KBr pellets (Aldrich, 99%, analytical reagent), the FT-IR spectra of the samples were recorded at room temperature. Using an X-ray diffractometer (X'pert PAnalytical Philips, Holland), with Cu K radiation line of wavelength 1.54 Å in 2θ range from 10° to 80°, the crystal phases were verified at 25 °C. The CuKα radiation source was adjusted at 40 kV voltage, 30 mA current, and 10°/min scanning speed. The TEM images of the nanocomposite were recorded on a Phillips EM 208S microscope at 100 kV.

https://doi.org/10.1021/acsomega.4c01608
ACS Omega 2024, 9, 27260−27268

RESULTS AND DISCUSSION

Characterization of GO/GONRs/CS Aerogels. The FT-IR spectra of GO, GONRs, and GO/GONRs/CS aerogel are shown in Figure 1. The FT-IR spectra of GO (Figure 1a) show

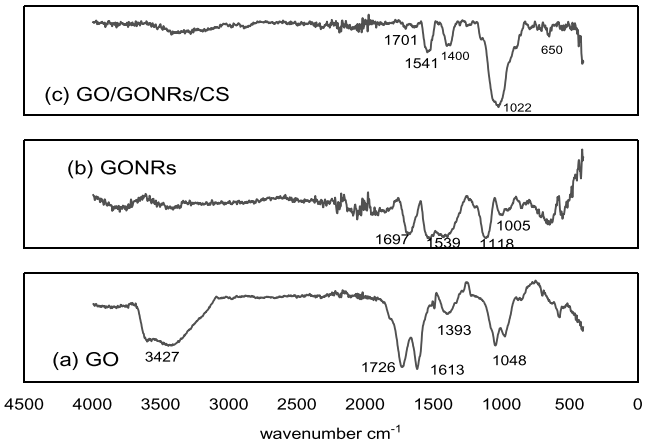

Figure 1. Spectra of FT-IR for GO (a), GONRs (b), and GO/GONRs/CS (c) aerogels.

characteristic peaks at 1621 cm^{-1} (C=C double bond) and 1393 cm^{-1} (indicating the bending vibrations of the groups −CH and $-CH_2$). Besides, the distinctive bands of GO are located near 1726, 1613, and 1048 cm^{-1}, which correspond to the stretching vibrations of the carbonyl C=O and double-bound C=C, as well as epoxy C−O. However, the broad peak with the value 3165−3501 cm^{-1} indicated −OH of the carboxylic group.[22−24] The FT-IR spectrum results for GONRs also showed a range of vibrational frequencies as shown in Figure 1b. GONRs exhibited characteristic peaks at 1539 cm^{-1} (double bond C=C), 2976 cm^{-1} (−CH and $-CH_2$ stretching vibrations), 1005, 1118 cm^{-1} (for C−O stretching vibration), and 1697 cm^{-1} (C=O stretching vibration).[17]

The FTIR results of the (GO/GONRs/CS) aerogel are shown in Figure 1c. The peaks of GONRs are shown at 1400, 1541 cm^{-1} (double bond C=C), 3192 cm^{-1} (O−H bending vibration for water adsorption), 1375 cm^{-1} (for −CH alkane bending), 2942 and 2872 cm^{-1} (−CH and $-CH_2$ stretching vibration), 1162 cm^{-1} (for C−O stretching vibration), and 1701 cm^{-1} (C=O stretching vibration). The GO/GONRs/CS composites revealed two new extra absorbance bands at 650 and 1022 cm^{-1}, which correspond to the C−O stretching vibrations of −NH and the −NHCO bending of $-NH_2$, respectively. This proves that CS was successfully grafted onto the GO/GONRs.[25,26]

Figure 2 displays the X-ray diffraction (XRD) spectra of GO, GONRs, and GO/GONRs/CS aerogels. The XRD spectra of GO are shown in Figure 2a. At 12.22°, the diffraction peaks formed, which corresponded to the characteristic peak of GO. The peak at 2θ = 12.22° of GO corresponded to the (001) crystal plane reflection of GO. Another peak was observed at 2θ = 43°, which belongs to the crystal plane (100).[27] The XRD structural characterization findings are displayed in Figure 2b. In GONRs, the (002) and (100) planes are responsible for the 25.0° and 43.0° diffraction peaks.[28] Figure 2c depicts the GO/GONRs/CS aerogel microspheres' XRD patterns 2. This composite's distinctive diffraction peak was seen at 2θ = 11°, along with a large peak for CS at 2θ = 20.37°. However, the GO/GONRs/CS aerogel microspheres' XRD patterns were

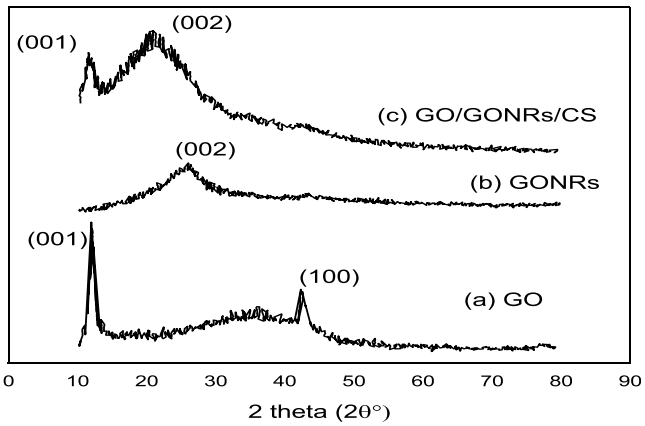

Figure 2. Patterns of XRD for (a) GO, (b) GONRs, and (c) GO/GONRs/CS aerogels.

almost identical to those of pure CS, and there was hardly any GO peak visible. This finding demonstrated that GO was not added to the GO/GONRs/CS aerogel microspheres, altering their amorphous structure. Therefore, rather of a chemical reaction between the CS and GO sheet, the sole physical contact (including van der Waals forces, hydrogen bonds, and $\pi-\pi$ stacking) may be to blame. Further, the addition of GO caused the diffraction intensity to drop and the peak at 2θ = 20.35° to expand, indicating that the amount of CS that was crystallized reduced as a result of the addition of GO.[29] In summary, the crystal structures of GO, GONRs, and GO/GONRs/CS aerogel microspheres are revealed by the XRD spectra, which also show the presence and configuration of each plane's crystal. The XRD patterns indicate that there is less CS crystallization in the composite material, indicating that the interaction between GO and CS is mostly physical rather than involving a chemical process.

Figure 3a indicates that GO has a two-dimensional sheet-like structure. The SEM pictures clearly show that GO has numerous lamellar layer structures and that the margins of individual sheets can be distinguished.[30] The films are layered one on top of the other and have wrinkled sections. It is also crucial to note that the GO sheets' borders are thicker. This is because the functional groups that include oxygen were mostly connected at the GO's boundaries. The SEM images displayed in Figure 3b demonstrate that the GONR sheets have a somewhat rougher surface and a larger ribbon structure. In addition, it is possible to note the porous shape formed by the graphene oxide ribbons, as well as the enlargement of the edges, which is due to the presence of functional aggregates, especially aggregates like carboxylic, hydroxyl, and epoxy groups.[31] The GO/GONRs/CS aerogel has a randomly distributed, interlinked, porous, and 3D structure, as shown in Figure 3c; the wrinkled sheets are spread out like a leaf and connected by continuous macropores. Zooming in on a single sheet reveals a chitosan surface with a smooth surface covered with graphene sheets.[32]

The TEM images, which are displayed in Figure 4, clearly illustrate the formation of graphene oxide sheets and ribbons as well as the fabrication of these materials by using chitosan and the creation of a triple network.

https://doi.org/10.1021/acsomega.4c01608
ACS Omega 2024, 9, 27260−27268

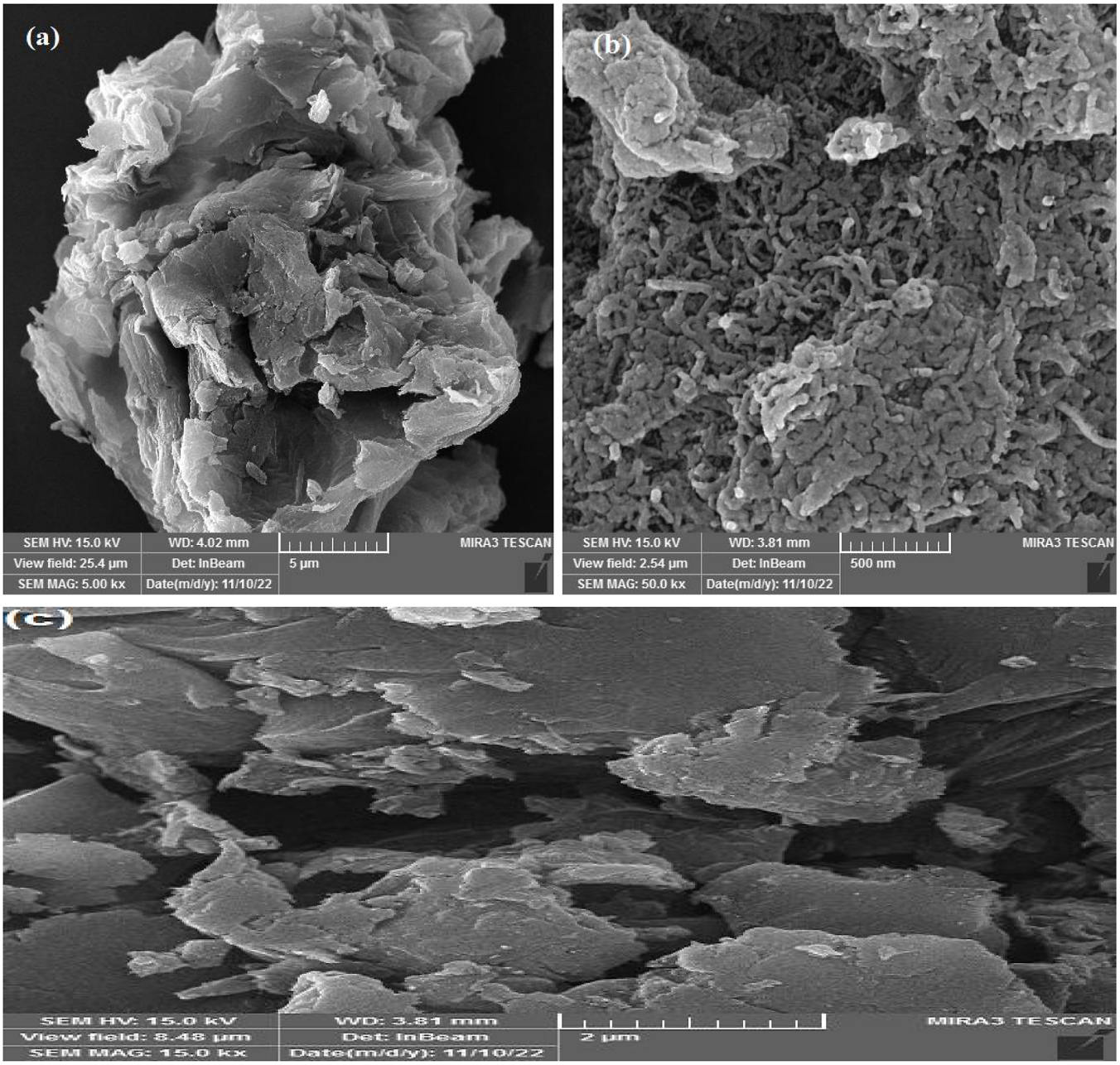

Figure 3. FESEM images of GO (a), GONRs (b), and GO/GONRs/CS (c) aerogels.

ADSORPTION OF URANIUM(VI) ON GO/GONRS/CS AEROGELS

Effect of Solid Dosage. According to Figure 5, the quantity of U(VI) that sorbs onto GO/GONRs/CS aerogels increased as the solid concentration increased. However, after adding 15 mg of sorbent, there were no discernible changes in the quantity of U(VI) adsorption on the GO/GONRs/CS aerogels. Therefore, the subsequent sorption studies employed 15 mg of sorbent. Using 15 mg of sorbent ensures that the maximum adsorption capacity of the aerogels is utilized without any excess sorbent, which allows for the efficient use of resources and avoids unnecessary wastage of the sorbent material. Additionally, using a fixed sorbent amount of 15 mg allows for consistent and comparable results in the subsequent sorption studies.[33]

Effect of pH. One of the most critical parameters that plays a significant effect in GO-based materials' uranium adsorption is pH. The pH value of solutions containing uranium could affect the surface charge of GO-based nanomaterials and the species of uranium in the solution, thereby influencing the interaction between these nanomaterials and uranium species and resulting in varying adsorption efficiencies at different pH values. It is evident from Figure 6 that the adsorption capacity of the adsorbent is highly dependent on the solution's pH value. At a low solution pH, a significant quantity of H^+ competes with uranyl cations for binding sites on the nanocomposite adsorbent surface, hence decreasing the uranium(VI) adsorption efficiency. Because the deprotonation process GO-based nanoparticles become negatively charged on their surface when the pH of the solution rises, positive uranyl ionic complexes such as $(UO_2)_3(OH)^{5+}$, $(UO_2)_2(OH)_2^{2+}$, and

https://doi.org/10.1021/acsomega.4c01608
ACS Omega 2024, 9, 27260−27268

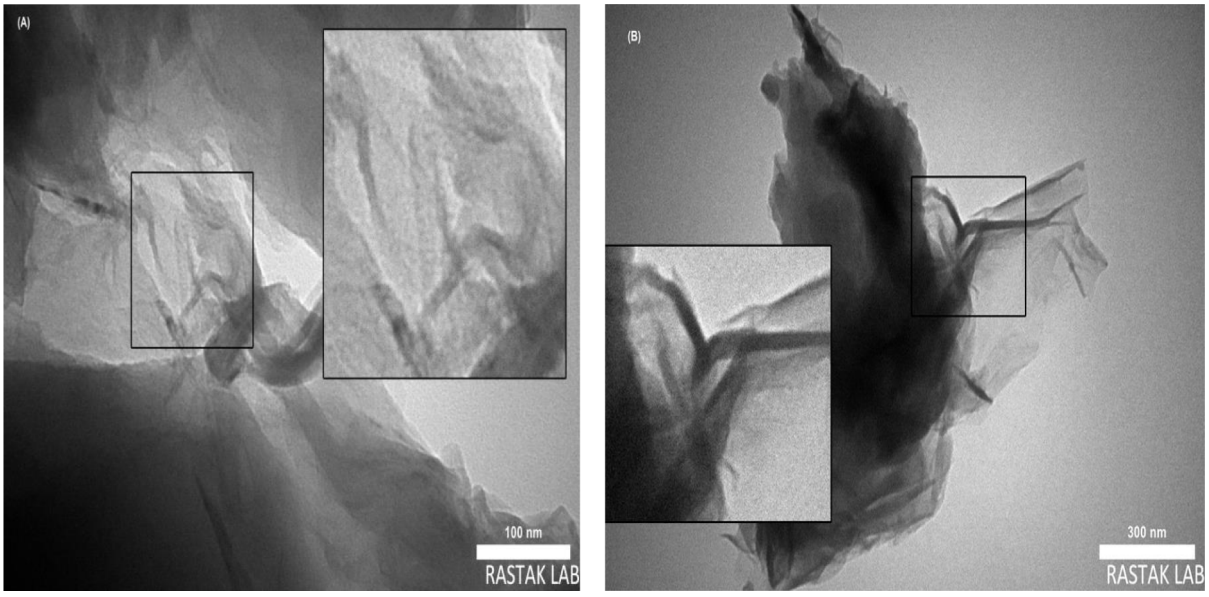

Figure 4. TEM images of GO/GONRs/CS: (a) 100 and (b) 300 nm

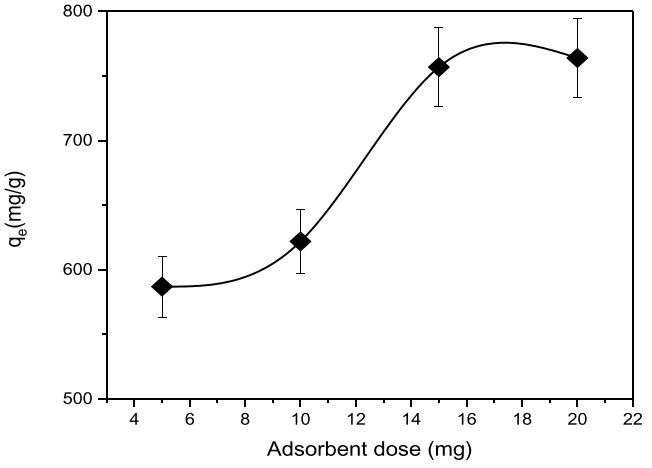

Figure 5. Solid dosage effect of the GO/GONRs/CS aerogel on the adsorption capacity at 313 K, 24 h, 250 mg/L of U, pH = 6.02.

UO_2OH^+, and are simultaneously produced, electrostatic interactions between the positively charged uranyl complexes and the negatively charged surface of composite as uranium adsorbents increase, hence enhancing the uranium adsorption efficiency. increasing the pH of the solution might cause uranium ions to hydrolyze, resulting in the production of anionic complexes such as $UO_2(CO_3)_3^{4-}$, $UO_2(CO_3)_2^{2-}$, $(UO_2)_3(OH)^{7-}$, UO_2 $(OH)^{3-}$, or $UO_2(OH)_2$ precipitation and, subsequently, a decrease in uranium adsorption efficiency. It was shown that the optimum pH for this adsorption is 6.

Adsorption Kinetics. According to Table 1 and Figure 7, 15 h is the optimal time to complete the adsorption process between the GO/GONRs/CS aerogel and uranium solution to attain complete equilibrium. The contact time necessary to attain adsorption equilibrium is a significant characteristic that reflects the adsorption capabilities of uranium adsorbates. Changes in adsorption capacity as a function of contact time characterize the adsorption dynamics. The large specific surface area and numerous functional groups on the surface of the aerogel play crucial roles in enhancing the adsorption

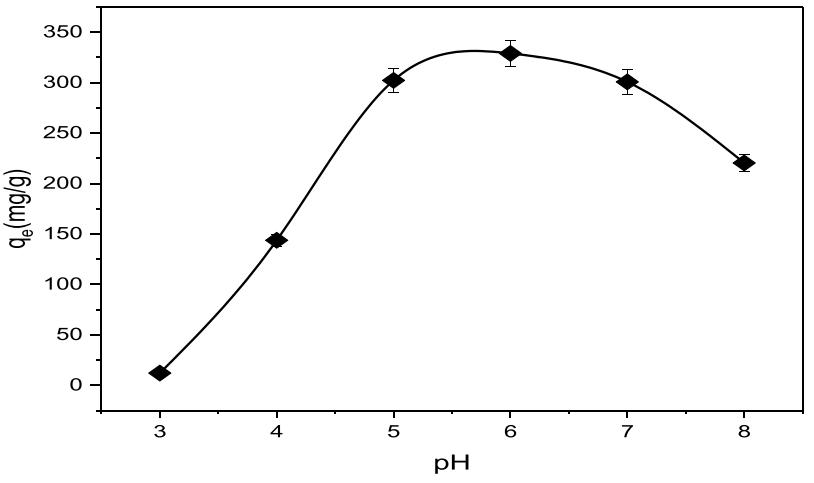

Figure 6. Effect of pH on adsorption capacity at 313 K, 24 h, mass of GO/GONRs/CS = 15 mg, conc. *U* = 100 mg/L.

https://doi.org/10.1021/acsomega.4c01608
ACS Omega 2024, 9, 27260−27268

Table 1. Kinetic Parameters of U(VI) Sorption on GO/GONRs/CS Aerogels

$q_{e,exp}$/(mg/g)	pseudo-first-order kinetics		
	$k_1/(h^{-1})$	$q_{e,cal}$/(mg/g)	R^2
750.329	0.29	285.89	0.8467
$q_{e,exp}$/(mg/g)	pseudo-second-order kinetics		
	$k_2/(g\ mg^{-1}\ h^{-1})$	$q_{e,cal}$/(mg/g)	R^2
750.329	0.001608	784.87	0.9989

rate of U(VI), and therefore the adsorption equilibrium of U(VI) on the aerogel may be reached rapidly.

Two alternative kinetic models—pseudo-first-order and pseudo-second order models—were employed to investigate the adsorption mechanism process. The following eqs 3 and 4, respectively, may be used to express the models.

$$\ln(q_e - q_t) = \ln q_e - k_1 \cdot t \tag{3}$$

$$\frac{t}{q_t} = \frac{1}{k_2 q_e^2} + \frac{t}{q_e} \tag{4}$$

where q_e (mg/g) is the quantity of U(VI) sorbed at equilibrium time and q_t (mg/g) is the amount of U(VI) sorbed at any time (h). The adsorption rate constants of pseudo-first-order and pseudo-second-order adsorption are denoted by k_1 (h^{-1}) and k_2 (g mg^{-1} h^{-1}), respectively.

The equations' important kinetic parameters were computed, and the results of k_1 and k_2 are reported in Table 1. As can be seen, the computed $q_{e,cal}$ value was so close to the experimental $q_{e,exp}$, suggesting that the pseudo-second-order model was better suited to represent the adsorption process of U(VI) on GO/GONRs/CS aerogels. Additionally, the pseudo-second-order model had the highest correlation coefficient (R^2) when compared to other kinetic models (pseudo-first-order).

Initial U(VI) Concentration Effect and Isotherm Studies. To understand the effect of the initial uranium concentration on adsorption, several experiments were conducted with uranium concentrations ranging from 50 to 350 mg/L. When the equilibrium concentration of U(VI) increased, so did the amount of U(VI) sorption on the GO/GONRs/CS aerogels. The maximal sorption quantity was discovered to be 1208.85 mg/g under the given testing circumstances.

Freundlich and Langmuir isotherm models were used to simulate the equilibrium sorption isotherms. According to the Langmuir isotherm model, sorption occurs on a homogeneous surface via monolayer adsorption, and there are no interactions between the neighboring binding sites of the adsorbates on the surface.[34] It may be written as eq 5.

$$\frac{C_e}{q_e} = \frac{1}{q_{max} K_L} + \frac{C_e}{q_{max}} \tag{5}$$

where C_e is the equilibrium concentration (mg/L), q_e is the sorbed quantity at equilibrium (mg/g), q_{max} (mg/g) refers to the adsorption capacity of the Langmuir monolayer, and the constant of equilibrium is K_L (L/mg).

The Freundlich isotherm model can be described as an actual correlation between the solute adsorption from a liquid surface and a solid surface. It presupposes the involvement of many sites with various sorption energies, and its linear form is provided by eq 6:

$$\ln q_e = \ln K_F + \frac{1}{n} \ln C_e \tag{6}$$

where K_F [(mg/g) $(L/mg)^{1/n}$] and n are the Freundlich constants that correspond to, respectively, the sorbent's capacity for sorption and the intensity of sorption.

The slopes and intercepts of the plots of C_e/q_e versus C_e and ln q_e versus ln C_e were used to compute the related parameters (Table 2). When R^2 values were compared, it was discovered that the Freundlich isotherm best described the sorption features of U(VI) on the GO/GONRs/CS aerogels.

Thermodynamic Studies. Sorption thermodynamics is an essential component to comprehend the energy change and establish whether the process might be spontaneous. Table 3 includes $\Delta G°$, $\Delta S°$, and $\Delta H°$ (thermodynamic parameters) of U(VI) adsorption in a hybrid aerogel. Table 3 shows that the sorption process is endothermic and spontaneous. Because of the positive values of $\Delta S°$, $\Delta H°$, and $\Delta G°$, high temperatures were preferred for the reaction.

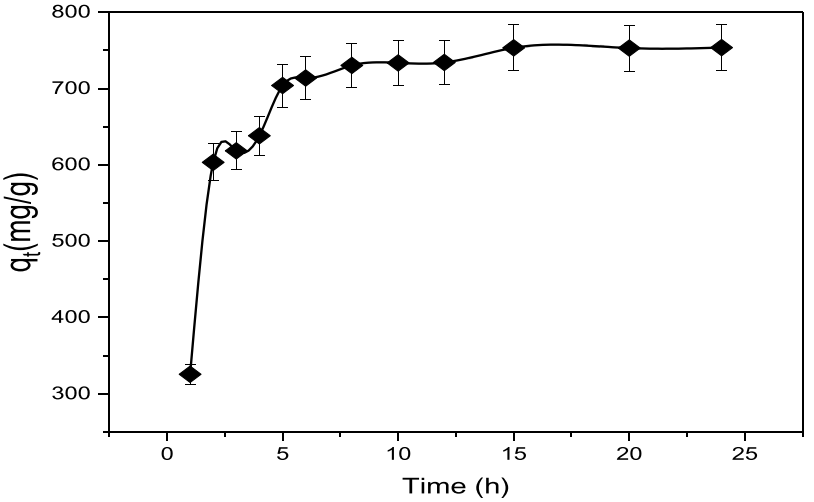

Figure 7. Relationship between the adsorption capacity and contact time at 313 K, pH 6.02, mass of GO/GONRs/CS = 15.2 mg, conc. U = 243 mg/L.

https://doi.org/10.1021/acsomega.4c01608
ACS Omega 2024, 9, 27260−27268

Table 2. Adsorption Isotherm Parameters of U(VI) Sorption on GO/GONRs/CS Aerogels

sorbent	Langmuir sorption isotherm			Freundlich sorption isotherm		
	q_{max}(mg g^{-1})	K_L(L mg^{-1})	R^2	K_F [(mg g^{-1})(L m^1)$^{1/n}$]	n	R^2
GO/GONRs/CS	1208.856	0.205	0.86	210.76	1.936	0.927

Table 3. Thermodynamic Parameters for U(VI) Adsorption on GO/GONRS/CS Aerogels

ΔH(kJ mol^{-1})	ΔS (J mol^{-1} K^{-1})	ΔG(kJ mol^{-1})	
12.182	62.513	−6.134	293 (K)
		−6.446	298 (K)
		−6.759	303 (K)
		−7.072	308 (K)
		−7.384	313 (K)

Equation 7 is used to calculate the change in the thermodynamic parameters of the sorption process.

$$\text{Ln } K_{eq} = \frac{-\Delta H}{RT} + \frac{\Delta S}{R} \quad (7)$$

K_{eq} represents the distribution coefficient (mL g^{-1}), whereas R represents the gas constant (8314 J mol^{-1} K^{-1}) and T represents the absolute temperature (K). ΔS is the entropy change (J mol^{-1} K^{-1}), and ΔH is the enthalpy change (kJ mol^{-1}). Eq 8 represents the change in Gibbs free-energy (ΔG) values (kJ mol^{-1}).

$$\Delta G^\circ = \Delta H^\circ - T\Delta S^\circ \quad (8)$$

The values of ΔH and ΔS in Table 3 were determined using the slope and intercept of the plots of ln K_{eq} versus T^{-1}, as opposed to eq 7. The endothermic nature of the adsorption process and the rise in randomness at the solid−solution interface during adsorption were shown by the positive values of ΔH and ΔS, respectively. The ΔG value progressively fell with the rising temperature until it was negative, showing that the sorption process was spontaneous in all of the investigated circumstances.

Comparison between GO/GONRs/CS Adsorbents and the Literature Studied. A comparison of the maximum adsorption of U(VI) onto various adsorbents under different experimental conditions is given in Table 4 for uranium. As seen, the maximum adsorption of U(VI) ions onto GO/GONRs/CS adsorbents is higher than that of the other reported adsorbents.

Table 4. Comparative Study of the U(VI) Adsorption Capabilities by GO/GONRs/CS with Different Known Adsorbents

adsorbent	adsorption capacity (mg/g)	ref
GO	99	35
GO-NH2	215.2	36
GONRs	394.1	37
GONRs/CS	320	8
GO-CS-AO	348.75	38
GO/GONRs	327.8	39
MAFP/GO/CS	260.58	40
CS/GO-4	271.2	41
COOH-GO-CTS	64.93	42
GO/GONRs/SA	929.16	14
GO/GONRs/CS	1208.85	This study

CONCLUSIONS

The conclusion provided effectively summarizes the key findings and implications of the study. It emphasizes the efficient adsorption of uranium from wastewater using graphene oxide/graphene oxide nanoribbons/chitosan aerogels. The study highlights the chemisorption mechanism, indicating strong chemical interactions between uranium ions and the functional groups on the aerogel surface. The high adsorption capacity of 1208.85 mg/g for U(VI) demonstrates the effectiveness of the aerogels in removing uranium from aqueous solutions. The study also acknowledges the unique physicochemical properties and functional groups of the graphene oxide-based nanomaterials, which contribute to their promising uranium adsorption capabilities. with an endothermic, spontaneous, and pH-dependent process. The combination of graphene oxide, GONRs, and chitosan in aerogels enhanced the adsorption capacity and hydrophobicity, making them effective in removing uranium from aqueous solutions. The adsorption process followed a pseudo-second-order kinetic model and was well described by the Freundlich model. The study highlights the potential of GO-based nanocomposites for efficient uranium adsorption in wastewater treatment.

AUTHOR INFORMATION

Corresponding Authors

Adel Kareem Jasim − *Department of Chemistry, College of Science, University of Misan, Amarah 62001 Maysan, Iraq*; Email: adelkarimmm@uomisan.edu.iq

Zaidon T. Al-aqbi − *Department of Chemistry, College of Science, University of Misan, Amarah 62001 Maysan, Iraq*; orcid.org/0000-0002-9578-4228; Email: zthal@utas.edu.au

Authors

Ali A. Jabbar − *College of Science/Chemistry Department, Mustansiriyah University, Baghdad 10052, Iraq*

Dhia H. Hussain − *College of Science/Chemistry Department, Mustansiriyah University, Baghdad 10052, Iraq*

Kamal H. Latif − *The Iraqi Authority for the Control of Radioactive Sources, Baghdad 10052, Iraq*

Hussein S. Alghannami − *Department of Physics, College of Science, University of Misan, Amarah 62001 Maysan, Iraq*

Abdulkarim Albishri − *Department of Chemistry, Rabigh College of Arts and Sciences, King Abdulaziz University, Jeddah 21589, Saudi Arabia*

Complete contact information is available at: https://pubs.acs.org/10.1021/acsomega.4c01608

Author Contributions

A.A.J., D.H.H., and K.H.L. conducted all experiments and wrote the main manuscript text. A.K.J., Z.T.A., H.S.A., and A.A. wrote the review and edited the manuscript. A.K.J. and Z.T.A. prepared the figures and tables of the paper. All authors reviewed the manuscript.

https://doi.org/10.1021/acsomega.4c01608
ACS Omega 2024, 9, 27260−27268

Funding
This research received no external funding.

Notes
The authors declare no competing financial interest.

■ ACKNOWLEDGMENTS

The authors extend their sincere thanks to the Iraqi Atomic Energy Commission, Directorate of Central Laboratories, for providing distinguished support for the success of this work.

■ REFERENCES

(1) Lourenço, J.; Marques, S.; Carvalho, F. P.; Oliveira, J.; Malta, M.; Santos, M.; Gonçalves, F.; Pereira, R.; Mendo, S. Uranium mining wastes: The use of the Fish Embryo Acute Toxicity Test (FET) test to evaluate toxicity and risk of environmental discharge. *Science of The Total Environment* **2017**, *605*−*606*, 391−404.
(2) Ochiai, A.; Imoto, J.; Suetake, M.; Komiya, T.; Furuki, G.; Ikehara, R.; Yamasaki, S.; Law, G. T. W.; Ohnuki, T.; Grambow, B.; Ewing, R. C.; Utsunomiya, S. Uranium Dioxides and Debris Fragments Released to the Environment with Cesium-Rich Microparticles from the Fukushima Daiichi Nuclear Power Plant. *Environ. Sci. Technol.* **2018**, *52* (5), 2586−2594.
(3) Rosenberg, E.; Pinson, G.; Tsosie, R.; Tutu, H.; Cukrowska, E. Uranium Remediation by Ion Exchange and Sorption Methods: A Critical Review. *Johnson Matthey Technology Review* **2016**, *60* (1), 59−77.
(4) Mehta, V. S.; Maillot, F.; Wang, Z.; Catalano, J. G.; Giammar, D. E. Effect of co-solutes on the products and solubility of uranium(VI) precipitated with phosphate. *Chem. Geol.* **2014**, *364*, 66−75.
(5) Sun, Q.; Aguila, B.; Perman, J.; Ivanov, A. S.; Bryantsev, V. S.; Earl, L. D.; Abney, C. W.; Wojtas, L.; Ma, S. Bio-inspired nano-traps for uranium extraction from seawater and recovery from nuclear waste. *Nat. Commun.* **2018**, *9* (1), 1644.
(6) Guo, X.; Yang, H.; Liu, Q.; Liu, J.; Chen, R.; Zhang, H.; Yu, J.; Zhang, M.; Li, R.; Wang, J. A chitosan-graphene oxide/ZIF foam with anti-biofouling ability for uranium recovery from seawater. *Chemical Engineering Journal* **2020**, *382*, No. 122850.
(7) Sheng, G.; Huang, C.; Chen, G.; Sheng, J.; Ren, X.; Hu, B.; Ma, J.; Wang, X.; Huang, Y.; Alsaedi, A.; Hayat, T. Adsorption and co-adsorption of graphene oxide and Ni(II) on iron oxides: A spectroscopic and microscopic investigation. *Environ. Pollut.* **2018**, *233*, 125−131.
(8) Hu, X.; Wang, Y.; Yang, J. O.; Li, Y.; Wu, P.; Zhang, H.; Yuan, D.; Liu, Y.; Wu, Z.; Liu, Z. Synthesis of graphene oxide nanoribbons/chitosan composite membranes for the removal of uranium from aqueous solutions. *Frontiers of Chemical Science and Engineering* **2020**, *14* (6), 1029−1038.
(9) Davies, R. V.; Kennedy, J.; McIlroy, R. W.; Spence, R.; Hill, K. M. Extraction of Uranium from Sea Water. *Nature* **1964**, *203* (4950), 1110−1115.
(10) Bai, J.; Chu, J.; Yin, X.; Wang, J.; Tian, W.; Huang, Q.; Jia, Z.; Wu, X.; Guo, H.; Qin, Z. Synthesis of amidoximated polyacrylonitrile nanoparticle/graphene composite hydrogel for selective uranium sorption from saline lake brine. *Chemical Engineering Journal* **2020**, *391*, No. 123553.
(11) Li, Z.; Chen, F.; Yuan, L.; Liu, Y.; Zhao, Y.; Chai, Z.; Shi, W. Uranium(VI) adsorption on graphene oxide nanosheets from aqueous solutions. *Chemical Engineering Journal* **2012**, *210*, 539−546.
(12) Peniche, C.; Argüelles-Monal, W.; Peniche, H.; Acosta, N. J. M. B. Chitosan: an attractive biocompatible polymer for microencapsulation. *Macromol. Sci.* **2003**, *3* (10), 511−520, DOI: 10.1002/mabi.200300019.
(13) Chen, Y.; Chen, L.; Bai, H.; Li, L. Graphene oxide−chitosan composite hydrogels as broad-spectrum adsorbents for water purification. *J. Mater. Chem. A* **2013**, *1* (6), 1992−2001, DOI: 10.1039/C2TA00406B.
(14) Jabbar, A. A.; Hussain, D. H.; Latif, K. H.; Albukhaty, S.; Jasim, A. K.; Sulaiman, G. M.; Abomughaid, M. M. Extremely efficient aerogels of graphene oxide/graphene oxide nanoribbons/sodium alginate for uranium removal from wastewater solution. *Sci. Rep.* **2024**, *14* (1), 1285.
(15) Ding, Y.; Zhu, J.; Wang, C.; Dai, B.; Li, Y.; Qin, Y.; Xu, F.; Peng, Q.; Yang, Z.; Bai, J.; Cao, W.; Yuan, Y.; Li, Y. Multifunctional three-dimensional graphene nanoribbons composite sponge. *Carbon* **2016**, *104*, 133−140.
(16) Wang, Y.; Wang, Z.; Gu, Z.; Yang, J.; Liao, J.; Yang, Y.; Liu, N.; Tang, J. J. J. O. R.; Chemistry, N. Uranium (VI) sorption on graphene oxide nanoribbons derived from unzipping of multiwalled carbon nanotubes. *J. Radioanal. Nucl. Chem.* **2015**, *304* (3), 1329−1337, DOI: 10.1007/s10967-015-3981-0.
(17) Hu, X.; Wang, Y.; Yang, J. O.; Li, Y.; Wu, P.; Zhang, H.; Yuan, D.; Liu, Y.; Wu, Z.; Liu, Z. Synthesis of graphene oxide nanoribbons/chitosan composite membranes for the removal of uranium from aqueous solutions. *Front. Chem. Sci. Eng.* **2020**, *14* (6), 1029−1038, DOI: 10.1007/s11705-019-1898-9.
(18) Wu, K.; Liu, X.; Li, Z.; Jiao, Y.; Zhou, C. Fabrication of chitosan/graphene oxide composite aerogel microspheres with high bilirubin removal performance. *Mater. Sci. Eng. C Mater. Biol. Appl.* **2020**, *106*, No. 110162.
(19) Guo, X.; Qu, L.; Zhu, S.; Tian, M.; Zhang, X.; Sun, K.; Tang, X. Preparation of Three-Dimensional Chitosan-Graphene Oxide Aerogel for Residue Oil Removal. *Water Environ. Res.* **2016**, *88* (8), 768−778.
(20) Sun, Z.; Chen, D.; Chen, B.; Kong, L.; Su, M. Enhanced uranium (VI) adsorption by chitosan modified phosphate rock. *Colloids, Surf., A* **2018**, *547*, 141−147, DOI: 10.1016/j.colsurfa.2018.02.043.
(21) Spoială, A.; Ilie, C.-I.; Ficai, D.; Ficai, A.; Andronescu, E. Chitosan-based nanocomposite polymeric membranes for water purification—A review. *Materials* **2021**, *14* (9), 2091 DOI: 10.3390/ma14092091.
(22) Sudesh, S.; Kumar, N.; Das, S.; Bernhard, C.; Varma, G. Effect of graphene oxide doping on superconducting properties of bulk MgB2. *Supercond. Sci. Technol.* **2013**, *26*, No. 095008.
(23) Sun, Z.; Fan, W.; Liu, T. Graphene/graphene nanoribbon aerogels as tunable three-dimensional framework for efficient hydrogen evolution reaction. *Electrochim. Acta* **2017**, *250*, 91−98.
(24) Wang, W.; Wu, Y.; Jiang, Z.; Wang, M.; Wu, Q.; Zhou, X.; Ge, X. Formation mechanism of 3D macroporous graphene aerogel in alcohol-water media under gamma-ray radiation. *Appl. Surf. Sci.* **2018**, *427*, 1144−1151.
(25) El Rouby, W.; Farghali, A. A.; Sadek, M.; Khalil, W. Fast removal of Sr (II) from water by graphene oxide and chitosan modified graphene oxide. *J. Inorg. Organomet. Polym.* **2018**, *28* (6), 2336−2349, DOI: 10.1007/s10904-018-0885-9.
(26) Liao, Y.; Wang, M.; Chen, D. Preparation of polydopamine-modified graphene oxide/chitosan aerogel for uranium (VI) adsorption. *Ind. Eng. Chem. Res.* **2018**, *57* (25), 8472−8483, DOI: 10.1021/acs.iecr.8b01745.
(27) Maharana, H.; Kumar Rai, P.; Basu, A. Surface-mechanical and electrical properties of pulse electrodeposited Cu−graphene oxide composite coating for electrical contacts. *J. Mater. Sci.* **2017**, *52*, 1089−1105, DOI: 10.1007/s10853-016-0405-7.
(28) Teles, R.; Arenillas, A.; da Silva, G.; Fernández, P.; Cardoso, E.; Maia, G.; Martins, C. Understanding the Influence of the Biomass-Derived Alcohols on the Activity and Stability of Pt Nanoparticles Supported on Graphene Nanoribbons. *Electrocatalysis* **2017**, *8*, 151−163, DOI: 10.1007/s12678-016-0349-3.
(29) Liu, L.; Li, C.; Bao, C.; Jia, Q.; Xiao, P.; Liu, X.; Zhang, Q. Preparation and characterization of chitosan/graphene oxide composites for the adsorption of Au (III) and Pd (II). *Talanta* **2012**, *93*, 350−357, DOI: 10.1016/j.talanta.2012.02.051.
(30) Alam, S. N.; Sharma, N.; Kumar, L. Synthesis of graphene oxide (GO) by modified hummers method and its thermal reduction to obtain reduced graphene oxide (rGO). *Graphene* **2017**, *6* (1), 1−18, DOI: 10.4236/graphene.2017.61001.
(31) Kazemi, M.; Niazi, A.; Yazdanipour, A. J. C. Solid-Phase Microextraction of Phthalate Esters from Aqueous Media by

https://doi.org/10.1021/acsomega.4c01608
ACS Omega 2024, 9, 27260−27268

Functionalized Carbon Nanotubes (Graphene Oxide Nanoribbons) and Determination by GC−FID. *Chromatographia* **2021**, *84* (6), 559−569, DOI: 10.1007/s10337-021-04032-z.
(32) Guo, X.; Qu, L.; Zhu, S.; Tian, M.; Zhang, X.; Sun, K.; Tang, X. Preparation of three-dimensional chitosan−graphene oxide aerogel for residue oil removal. *Water Environ. Res.* **2016**, *88* (8), 768−778, DOI: 10.2175/106143016X14609975747207.
(33) Zou, H.; Zhou, L.; Huang, Z.; Liu, Z.; Luo, T. Characteristics of equilibrium and kinetic for U (VI) adsorption using novel diamine-functionalized hollow silica microspheres. *J. Radioanal. Nucl. Chem.* **2017**, *311* (1), 269−278, DOI: 10.1007/s10967-016-4937-8.
(34) Geng, J.; Ma, L.; Wang, H.; Liu, J.; Bai, C.; Song, Q.; Li, J.; Hou, M.; Li, S. Nanotechnology, Amidoxime-grafted hydrothermal carbon microspheres for highly selective separation of uranium. *J. Nanosci. Nanotechnol.* **2012**, *12* (9), 7354−7363, DOI: 10.1166/jnn.2012.6518.
(35) Wang, X.; Chen, Z.; Wang, X. Graphene oxides for simultaneous highly efficient removal of trace level radionuclides from aqueous solutions. *Sci. China Chem.* **2015**, *58*, 1766−1773, DOI: 10.1007/s11426-015-5435-5.
(36) Liu, S.; Li, S.; Zhang, H.; Wu, L.; Sun, L.; Ma, J. Removal of uranium(VI) from aqueous solution using graphene oxide and its amine-functionalized composite. *J. Radioanal. Nucl. Chem.* **2016**, *309* (2), 607−614.
(37) Wang, Y.; Wang, Z.; Gu, Z.; Yang, J.; Liao, J.; Yang, Y.; Liu, N.; Tang, J. Uranium(VI) sorption on graphene oxide nanoribbons derived from unzipping of multiwalled carbon nanotubes. *Journal of Radioanalytical and Nuclear Chemistry* **2015**, *304* (3), 1329−1337.
(38) Yang, S.; Huang, Y.; Huang, G.; Peng, W.; Guo, C.; Shi, J. Preparation of amidoxime-functionalized biopolymer/graphene oxide gels and their application in selective adsorption separation of U(VI) from aqueous solution. *Journal of Radioanalytical and Nuclear Chemistry* **2020**, *324* (2), 847−855.
(39) Hu, X.; Wang, Y.; Wu, P.; Li, Y.; Tu, H.; Wang, C.; Yuan, D.; Liu, Y.; Cao, X.; Liu, Z. Preparation of graphene/graphene nanoribbons hybrid aerogel and its application for the removal of uranium from aqueous solutions. *Journal of Radioanalytical and Nuclear Chemistry* **2020**, *325* (1), 207−215.
(40) Ren, Q.; Xia, H.; Wang, Y.; Lv, J.; Yuan, D.; Liu, Y.; Zhou, L.; Li, Y.; Wang, Y. Novel malonamide-amidoxime bifunctional polymers decorated graphene oxide/chitosan electrode for enhancing electrosorptive removal of uranium(VI). *Sep. Purif. Technol.* **2024**, *330*, No. 125292.
(41) Liu, Y.; Tang, X.; Zhou, L.; Liu, Z.; Ouyang, J.; Dai, Y.; Le, Z.; Adesina, A. A. Nanofabricated chitosan/graphene oxide electrodes for enhancing electrosorptive removal of U(VI) from aqueous solution. *Sep. Purif. Technol.* **2022**, *290*, No. 120827.
(42) Patel, K.; Sutar, A. K.; Maharana, T. Microwave-assisted preparation of carboxylic graphene oxide-chitosan composite for adsorption of uranium and heavy toxic metals in water samples. *Sep. Sci. Technol.* **2022**, *57* (14), 2242−2260.

https://doi.org/10.1021/acsomega.4c01608
ACS Omega 2024, 9, 27260−27268